Scientific Research and Essays Vol. 6(6), pp. 1209-1215, 18 March, 2011
Available online at http://www.academicjournals.org/SRE
DOI: 10.5897/SRE10.572
ISSN 1992-2248 ©2011 Academic Journals

Full Length Research Paper

Estimation of specific absorption rate and temperature increases in the human head due to portable telephones

Mohammad Rashed Iqbal Faruque[1,2]*, Norbahiah Misran[1,2], Rosdiadee Nordin[2], Mohammad Tariqul Islam[1] and Baharudin Yatim[1]

[1]Faculty of Engineering and Built Environment, Institute of Space Science (ANGKASA), Universiti Kebangsaan Malaysia, 43600 UKM, Bangi, Selangor, Malaysia.
[2]Depatment of Electrical, Electronic and Systems Engineering, Faculty of Engineering and Built Environment Building, Universiti Kebangsaan Malaysia, 43600 UKM, Bangi, Selangor, Malaysia.

Accepted 28 February, 2011

The bioheat equation is solved for an anatomically based model of the human head with a resolution of 2.5 × 2.5 × 2.5 mm to study the thermal implications of exposure to electromagnetic (EM) fields typical of cellular telephones at 900 MHz. Attention has first been posed on a particular phone model, and a comparison between the absorbed power distribution and steady-state temperature increases has been carried out. The antenna output power was set to be consistent with the portable telephones of 600 mW, maximum SAR values, averaged over 1 gm, from 2.1 to 3.6 W/kg depending on the considered phone. The maximum temperature increases are obtained in the ear and vary from 0.22°C to 0.39°C, while the maximum temperature increases in the brain lie from 0.07°C to 0.17°C. These steady-state temperature increases are obtained after about 48 min of exposure, with a time constant of approximately 6 min. Application of the ANSI/IEEE safety guidelines restricting the 1 gm averaged spatial peak SAR to 1.6 W/kg results in the maximum temperature rise in the brain from 0.07°C to 0.15°C at 900 MHz. Finally, considerations about the exposure limits in the considered studied frequency are made.

Key words: Electromagnetic wave polarization, electromagnetic heating, finite-difference time-domain method, mobile phone, specific absorption rate, temperature increase.

INTRODUCTION

Much attention has been paid to the health implications of electromagnetic (EM) wave in the last 20 years. Mobile telephones are singled out since they have been spread rapidly and are used in close proximity to the user's head. The assessment of the power absorbed in the user's head is a key task, both for design and acquiescence testing of mobile phones, which can be efficiently performed numerically. At present, among the numerical techniques, the most often applied in the presence of highly non-homogeneous structures, like the human head, is the finite-difference time-domain (FDTD) method, thanks to its efficiency and simplicity of implementation (Kunz and Luebbers, 1993; Taflove, 1995; Islam et al., 2009a, b). In fact, when a cellular phone is working, the transmitting antenna is placed very close to the user's head where a substantial part of the radiated power is absorbed. Up till now, the most recognized RF exposure standards adopt the SAR, averaged over the whole body (SAR_{WB}), as the basic parameter to establish the safety of an exposure (IEEE, 2005; ICNIRP, 1998). The value of 4 W/kg is accepted worldwide as the threshold for the induction of biological thermal effects. In the setting up of RF standards, a safety factor of 50 for general public (or uncontrolled) exposure has been introduced, giving rise to a basic limit on SAR_{WB} equal to 0.08 W/kg. When the power absorption takes place in a confined body region, as in the case of the head exposed to a cellular phone, even if the SAR_{WB} is well below the basic limit, the local SAR can assume rather high values. For this reason, limits on local SAR averaged over tissue masses of 1 or 10 g have been introduced in the standards. These local limits have

*Corresponding author. E-mail: rashedgen@yahoo.com.

been chosen, increasing the basic limit on SAR_{WB} of a factor from 20 to 25, giving rise to the well-known values of 1.6 W/kg over 1 g (Kunz et al., 1993; Taflove, 1995) or 2 W/kg over 10 g (ICNIRP, 1998).

Numerical dosimetry applied to the problem of human head exposure to fields radiated by mobile phones exhaustively answered many questions, but some problems are still open. In particular, one of them is the evaluation of induced temperature increases in the user's head, which can be directly compared with the thresholds for the induction of known adverse thermal effects in the human head. Unfortunately, even if much has been done in the field of numerical dosimetry, only a few papers are available addressing the EM-field/human-body interaction problem also from a thermal point of view (Wang and Fujiwara, 1999; Schmid et al., 2007; Faruque et al., 2010a). In particular, in all these studies, power deposition and temperature increase in the head of a cellular phone user have been evaluated only for cellular phone equipped with linear or planar antennas. Moreover, the above-cited studies have mainly considered the heating effect due to the SAR.

Therefore, a thermal investigation seems to be necessary, in addition to SAR analysis, to evaluate the safety of an exposure. In particular, in Handerson and Joyner, (1995), Islam et al. (2010), and Faruque et al. (2010b), starting from SAR values measured in a phantom head bare to handheld mobile phones, steady-state temperature rises were calculated, using a simplified thermal model for the brain, while in Lu et al. (1996), the attention was focused on a human head under plane-wave exposure. Studying the bioelectromagnetic interaction from a thermal point-of-view, it is interesting to compare the obtained temperature increases with the thresholds for the induction of thermal damages. The threshold temperature increase for neuron damage is about 4.5°C (for more than 30 min) (Schmid et al., 2007; Bernardi et al., 2000).

Experiments performed on the eye have evidenced a threshold increase of 3 to 5°C in the lens for the induction of the cataract (Guyton, 2010; Hirata and Fujiwara, 2009). The temperature increase necessary to induce thermal damage in the skin is at least 10°C (Sliney and Stuck, 1994; Kwon et al., 2009). Finally, experiments performed on animals have evidenced various physiological effects when the body core temperature rises more than 1 to 2°C (ICNIRP, 1998). However, in practical situations, two more causes for temperature increases are present. The first one is the contact between the phone case and the user's head (in particular, ear and cheek) that block the convective heat exchange between the skin layers and air, causing temperature rises in the tissues around the contact zone. Obviously, this heating is totally independent from the radiated power and, indeed, it can also be observed for a wire line phone. The second additional cause for temperature increase in the heating of the phone itself, due to the power debauched in the circuitry and, in particular, in the power amplifier; this heating is transmitted to the head tissues via thermal conduction. In this work, we have evaluated the power absorption and the corresponding temperature increases induced in an anatomical heterogeneous model of the human head exposed to the field emitted by a portable phone operating around 900 MHz.

MODEL AND METHODS

The whole process of simulating the temperature distribution is indicated in Figure 1. The first step was the construction of a realistic anatomy. 3D magnetic resonance angiography scans (Philips Gyroscan, resolution better than 1 mm cubic) were made from one side of the head of an adult male volunteer. The three-dimensional anatomy describing the spatial distribution of the tissue types was constructed from a T1 weighted magnetic resonance imaging (MRI) image acquired concurrently with the magnetic resonance angiogram (MRA) images. The tissue segmentation was carried out using thresholding and binary erosion and dilation functions, with ample instruction manual intercession. In this paper, we investigate the SAR distributions in an anatomically based human head for plane wave exposure with the use of the FDTD method. The FDTD has been applied in its classical formulation (Kunz and Luebbers, 1993; Taflove, 1995) with second-order absorbing boundary conditions (Sliney and Stuck, 1994). Starting from the evaluated SAR distribution, the thermal response as a function of time, until the steady state is reached, has been calculated through an explicit finite-difference formulation of the bioheat equation. The power radiated in free space from the various types of telephones has been computed both on the basis of the feed point impedance and Poynting's vector flow obtaining a good agreement between the two.

The generator impedance has been assumed matched to the antenna free-space radiation impedance, with voltage amplitude suitable to obtain a radiated power of 600 mW in free space. It should be noted that when analyzing the coupling between a phone and human head, the radiated power decreases due to the change of the antenna radiation impedance (Flyckt et al., 2007). The SAR values averaged over 1 g (SAR 1 g) and over 10 gm (SAR 10 g) have been computed considering tissue masses in the shape of a cube with a volume of approximately 1 and 10 cm, respectively. Only cubes weighting at least 0.8 g for SAR 1g and 8 g for SAR 10 g have been examined.

RESULTS

The analysis and comparison of the SAR values and distributions for a particular phone model with the corresponding temperature increases (ΔT) has been presented in this paper. The disclosure of the head to a phone equipped with a patch antenna has been chosen as a reference situation. The phone is placed in the cheek position and its case is kept in direct contact with the ear. This gives rise to a distance of about 1.1 cm between the antenna feed point and the external part of the ear. The reference free-space radiated power is chosen as 600 mW for the analogue phone, whereas, the radiated power of digital generation of GSM cell phone 250 mW at 900 MHz. That is because the main aim of this article is to calculate the maximum temperature

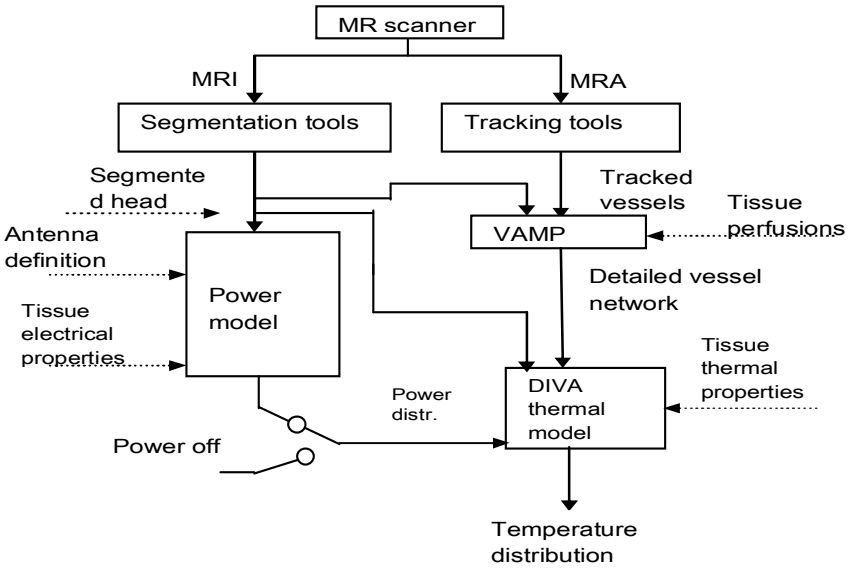

Figure 1. Flowchart describing the data flow (arrows) and tools (blocks) involved in the calculation of the temperature distribution in the human head resulting from RF radiation emitted by the antenna.

Table 1. Total power absorbed in the head (P_{abs}), maximum SAR as averaged over 1 g ($SAR_{1\,MAX}$) and 10 g ($SAR_{10\,MAX}$) of tissue in the head, and maximum SAR as averaged over 1 g of brain and tilted (T), power radiated in free space: 600 mW. Frequency: 900 MHz. Phone Position: C (Cheek); T (Tilted).

Phone model	Position	P_{abs} (mW)	SAR_{1MAX} (W/kg)	SAR_{10MAX} (W/kg)	$SAR_{1MAXbrain}$ (W/kg)	$SAR_{1MAXeye}$ (W/kg)
Patch	C	309	2.27	1.12	0.91	0.031
	T	268	2.28	1.23	0.64	0.056
Monopole	C	363	2.14	1.25	1.19	0.018
	T	327	2.37	1.26	0.72	0.074
Dipole	C	383	2.68	1.91	1.83	0.019
	T	325	2.81	1.07	0.83	0.013
PIFA	C	423	3.62	1.82	1.19	0.068
	T	405	3.37	1.96	1.27	0.161

values in human head tissues due to the possible maximum RF emission for the purpose of comparison with previously published works on this subject. Moreover, and although the IEEE C 95.1:2005 and FCC standards apply the SAR limit for the extremities to the normal pinnae, and since the used MRI-based head model has pressed pinnae; in this article, the pinnae are subject to the same exposure limit, for the SAR, as the head. It was observed that there were no substantial differences between the computed SAR values for the head with and without pressed pinnae, and the spatial-peak SAR location was not at the pinna, but instead the peak shift to region near the pinna (Zygirdis and Tsiboukis, 2008). Besides that the two causes of temperature increase in the head mentioned earlier (namely, SAR deposition and handset contact with ear and cheek skin), a third additional cause for the temperature increase is the heating of the handset itself. This is due to the power dissipated in the circuitry and, in particular, in the power amplifier; this heating is transferred to the head tissues via thermal conduction.

The results obtained are shown in the first row of Table 1 (as concerns SAR values) and of Table 2 (ΔT values). When the head is present, the radiated power decreases to 571 mW and more than 52% of this power (309 mW) is absorbed in the head (P_{abs}). The maximum $SAR_{1\,g}$ (SAR_{1Max}) and $SAR_{10\,g}$ (SAR_{10Max}) values are 2.27 and 1.12 W/kg, respectively. The maximum SAR in the brain, as averaged over 1 g ($SAR_{1Maxbrain}$), is 0.91 W/kg, and finally, a maximum 1 g averaged SAR of 0.031 W/kg is

Table 2. Steady-state temperature rise, maximum in the whole head (ΔT_{MAX}), in the brain ($\Delta T_{MAXbrain}$), and in the lens ($\Delta T_{MAXlens}$), phone positions: cheek (C) and tilted (T), power radiated in free space: 600 mW, frequency: 900 MHz.

Phone model	Position	ΔT_{MAX} (°C)	$\Delta T_{MAXbrain}$ (°C)	$\Delta T_{MAXlens}$ (°C)
Patch	C	0.22	0.11	0.004
	T	0.23	0.07	0.008
Monopole	C	0.22	0.12	0.003
	T	0.22	0.08	0.009
Dipole	C	0.31	0.17	0.003
	T	0.26	0.11	0.002
PIFA	C	0.39	0.12	0.01
	T	0.37	0.15	0.021

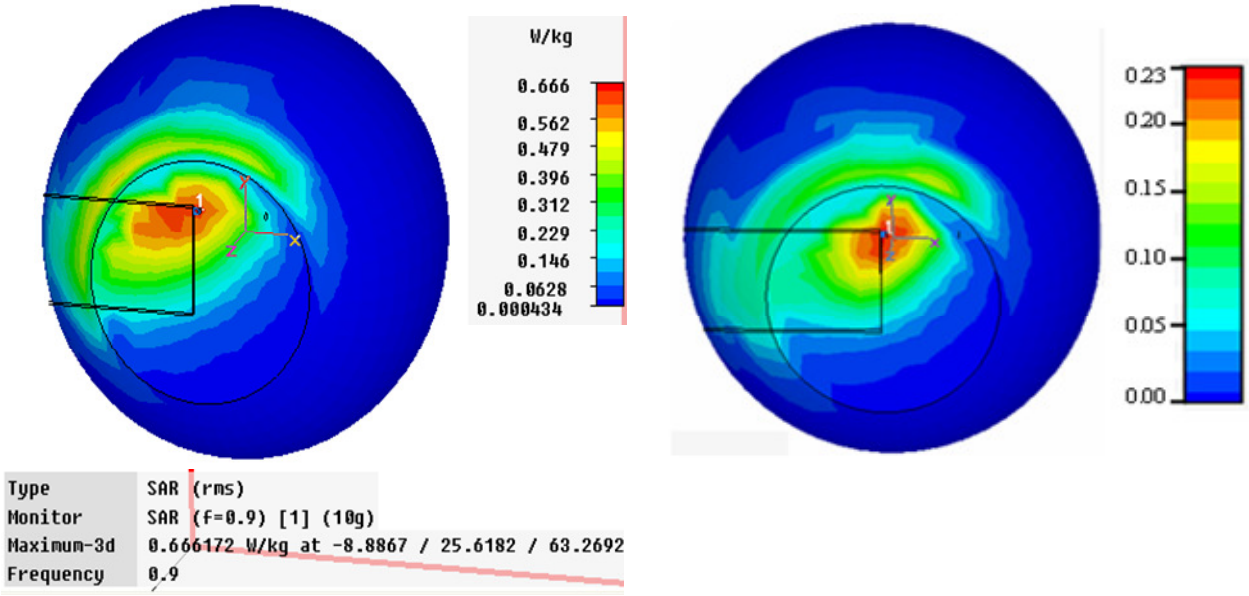

Figure 2. Front section of the head in which the maximum local SAR occurs for a patch phone in the cheek position. a) SAR distribution and b) Temperature increase distribution. Power radiated in free space: 600 mW. Frequency: 900 MHz.

obtained in the eye (SAR $_{1Maxeye}$). Figure 2a shows the SAR distribution evaluated on the cheek section of the head in which the maximum SAR occurs. Figure 2b shows the heating distribution in the same section as Figure 2a. From Figure 2b, it appears that the region where the maximum temperature increase takes place is located in the lower part of the ear. Figure 3a shows, for different call durations, the temperature increase in the point inside the ear where ΔT_{MAX} occurs. In Figure 3b, the corresponding evolution is reported for the ΔT_{MAX} point. In particular, exposures lasting 1, 3, 6, and 15 min are shown in the Figures.

DISCUSSION

For the considered phone, the SAR $_{1Max}$ and SAR $_{1Maxbrain}$ values are very close to those obtained in Dimbylow and Mann, (1994) and Tinniswood et al. (1998) in similar exposure conditions. Lower values were found in Buccella et al. (2007) with a different head model and with the antenna placed at a higher distance from the head. Higher values can also be found in the literature (Hombach et al., 1996; Zygirdis and Tsiboukis, 2008). The observed variability is essentially due to differences in phone geometry and position and in the used head

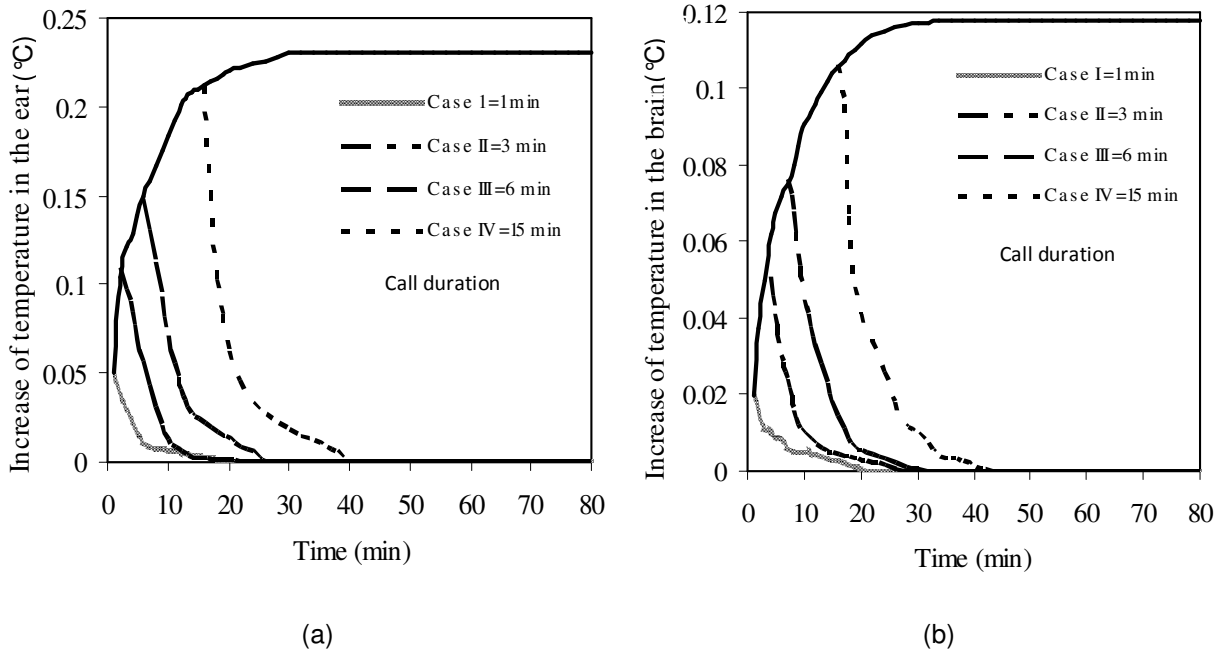

Figure 3. Time progression of the temperature increases for exposures for different cases where the maximum local ΔT occurs. (a) Inside the ear and (b) In the brain.

model. It can be noted that the highest SAR values are obtained in the central region of the ear that is in direct contact with the upper part of the phone case. From the Figure 2a, it appears that a certain amount of power absorption also takes place in the head region placed in front of the patch antenna, and in the lower part of the head (jaw, neck, and parotid gland) close to the radio case, which is part of the radiating structure. With reference to the thermal problem, first of all, the initial temperature distribution has been evaluated solving the bioheat equation in the non-irradiated head by using the *K, A*$_0$, and *B* values in this paper. The obtained distribution compares well with the physiological one (Scarella et al., 2006). After that, the temperature evolution has been evaluated taking into account the power absorption due to the field radiated by the phone. When the steady state is reached, the temperature rise (ΔT) is computed. Following this procedure, the maximum temperature rise (ΔT_{MAX}) is obtained in the ear region and is equal to 0.22°C. A temperature rise of 0.11°C is present in the external part of the brain close to the phone ($\Delta T_{Maxbrain}$). Finally, a negligible temperature variation is observed in the eye lens ($\Delta T_{Maxlens}$= 0.004°C).

Considering the results for $SAR_{1MAXbrain}$ and $\Delta T_{Maxbrain}$ it was noted that a temperature rise of 0.11°C was induced by a local dissipation of 0.91 W/kg. This corresponds to a normalized heating factor (ΔT /SAR_{1g}) of about 0.12°C/(W/kg). In the same exposure condition, the normalized heating factor in the inner brain is 0.03°C/(W/kg), which is more than four times lower. This different behavior is due to the fact that the maximum SAR and temperature increase in the brain are induced in the external part and not in the inner one. Consequently, since the external brain region is partly bounded by low blood perfusion and low thermal conductivity tissues (bone and fat), the cooling mechanism is less effective. The previous considerations clearly indicate that the presence of heterogeneous tissues greatly influences the temperature increases in the brain region, and that temperature increases are not directly proportional to the local SAR values, thus confirming the importance of using a complete thermal model. The comparisons between cheek and tilted position show that SAR and ΔT distributions are rather different. Due to the thermal conduction mechanism, the thermal profiles penetrates to a great extent in the ear region, while the high blood perfusion present in the brain, bringing away a great amount of heat, limits the temperature rise in the upper part of the head. The aforementioned reported thermal results refer to steady-state conditions, reached after about 48 min of disclosure (however, 90% of the final ΔT is reached after about 15 min) but previously, some researchers found that thermal results reach to steady-state conditions after 50 min of disclosure (Bernardi et al., 2000). This is because that in our research and their research, we used different antennas.

It should be noted that a phone call usually lasts a few minutes; hence, the steady-state temperature rise is rarely reached. It is, therefore, interesting to consider the time evolution of the temperature in some significant points. The rising part of the curves in Figures 3a and b can be approximated with a single exponential

expression of the kind $\Delta T_{MAX}(1\text{-}\exp(-t/\tau))$. The evaluation of the time constant is straightforward and a τ value of about 6 min has been obtained for both curves. It must be examined that the above-described temperature rises are due to the power deposition induced by the field radiated by the cellular phone. Anyhow, in practical situations, two more causes for temperature increase could be present. The first is the contact between the phone case and the ear that alters thermal exchange between the skin layers and the air, causing temperature rises in the tissues around the ear. The second is the heating up of the phone itself, due to the power debauched in the circuitry and, in particular, in the power amplifier; this heating is transmitted to the head tissues via thermal conduction. The influence of these two causes has been investigated by using the explicit finite-difference formulation of the bioheat equation. In particular, the investigation has been performed neglecting the SAR induced inside the head and considering both the contact between the phone and ear and the debauchery in the power amplifier (simulated adding a power deposition of 600 mW inside the upper part of the phone, corresponding to 50% efficiency).

Under these conditions, and after 15 min, a temperature increase of about 1°C is obtained in the ear, while the temperature increase in the brain region closest to the ear remains below 0.04°C. In conclusion, in the realistic use conditions, the heating of the ear seems to be mainly due to the phone contact and phone self-heating, while the SAR due to the field radiated by the phone plays an important role in the external brain heating.

CONCLUSIONS

The health hazards are mainly due to a temperature rise in tissue for RF exposure. The effect of localized SAR for cellular telephones should also be related to the temperature rise in the head. From this point of view, the temperature rise in the human head for portable telephones has been computed with an anatomically based human head model. The SAR in the human head has been determined using the FDTD method, and a bioheat equation has been numerically solved also using the FDTD method. With antenna output powers of 600 mW at 900 MHz in free space, that is typical of analog cellular phones. The new digital generation is characterized by a lower mean radiated power (250 mW). This means that the reported results should be decreased by a factor of 2.4, giving rise to SAR_{1MAX} values below the IEEE limit for all the considered phones. The temperature increases calculated in this study with a radiated power of 600 mW are at least 20 times lower than those indicated in the literature as thresholds for the induction of thermal damage.

It is fascinating to note that, for all the considered phone models, a maximum SAR_{1gm} value of 1.6 W/kg gives rise to a temperature increase in the brain of about 0.08°C, which is about 50 times lower than the threshold for thermal damage, while considering the ICNIRP limit of 2 W/kg averaged over 10 g, the brain heating is of about 0.2°C. These results exclude the possibility of thermally induced brain-tissue damage from cellular phones.

REFERENCES

Bernardi P, Cavagnaro M, Pisa S, Piuzzi E (2000). Specific absorption rate and temperature increases in the head of a cellular phone user. IEEE Trans. Microwave Theory Techniques, 48 (7): 1118-1126.

Buccella C, Santis VD, Feliziani M (2007). Prediction of temperature increases in human eyes due to RF sources. IEEE Trans. Electromagn. Compati., 49: 825-833.

Dimbylow PJ, Mann SM (1994). SAR calculations in an anatomically realistic model of the head for mobile communication transceivers at 900 MHz and 1.8 GHz. Phys. Med. Biol., 39: 1537-1553.

Faruque MRI, Islam MT, Misran N (2010a). Effect of human head shapes for mobile phone exposure on electromagnetic absorption. Informacije MIDEM, 40(3) (In Press).

Faruque MRI, Islam MT, Misran N (2010b). Evaluation of specific absorption rate (SAR) reduction for PIFA antenna using Metamaterials. Frequenz J., 64(7-8): 144-149.

Flyckt VM, Raaymakers MBW, Kroeze H, Lagendijk JJW (2007). Calculation of SAR and temperature rise in a high- resolution vascularized model of the human eye and orbit when exposed to a dipole antenna at 900, 1500 and 1800 MHz. Phys. Med. Biol., 52: 2691-2701.

Guyton AC (2010). Textbook of medical physiology. Philadelphia, 12th edition, PA: Saunders, pp. 1626-1629.

Handerson V, Joyner KH (1995). Specific absorption rate levels measured in a phantom head exposed to radio frequency transmission from analog hand-held mobile phones. Bioelectromag., 16: 60-69.

Hirata A, Fujiwara O (2009). The correlation between mass-averaged SAR and temperature elevation in the human head model exposed to RF near fields from 1 to 6 GHz. Phys. Med. Biol., 54: 7227-38.

Hombach V, Meier K, Burkhardt M, Kuhn E, Kuster N (1996) The dependence of EM energy absorption upon human head modeling at 900 MHz. IEEE Trans. Microwave Theory Tech., 44: 1865-1873.

ICNIRP Guidelines (1998). Guidelines for limiting exposure to time-varying electric, magnetic, and electromagnetic fields (up to 300 GHz), Health Phys., 74(4): 494-522.

IEEE Standard C 95.1–2005 (2005). IEEE standard for safety levels with respect to human exposure to radio frequency electromagnetic fields, 3 kHz to 300 GHz.

Islam MT, Faruque MRI, Misran N (2010). Study of specific absorption rate (SAR) in the human head by metamaterial attachment. IEICE Electronics Express., 7(4): 240-246.

Islam MT, Faruque MRI, Misran N (2009a). Design analysis of ferrite sheet attachment for SAR reduction in human head. Progress In Electromagnetics Research, PIER, 98: 191-205.

Islam MT, Faruque MRI, Misran N (2009b). Reduction of specific absorption rate (SAR) in the human head with ferrite material and Metamaterial. Progress In Electromagnetics Research, PIER C., 9: 47-58.

Kunz KS, Luebbers RJ (1993). The Finite difference time domain method for electromagnetics. Boca Raton, FL: CRC Press, pp. 35-53.

Lu Y, Ying J, Tan T, Arichandran K (1996). Electromagnetic and thermal simulations of 3-D human head model under RF radiation by using the FDTD and FD approaches, IEEE Trans. Magn., 42: 1653-1656.

Kwon MS, Huotilainen M, Shestakova A, Kujala T, Tanen RN, Hamalainen H (2009). No effects of mobile phone use or cortical auditory change-detection in children: An ERP study. Bioelectromagn,, 31(3): 191-199.

Scarella G, Clatz O, Lanter Si, Beaume G, Oudot S, Pons JP, Piperno S, Joly P, Wiart J (2006). Realistic numerical modeling of human head tissue exposure to electromagnetic waves from cellular phones, C. R. Physique (Elsevier)., 7: 501-508.

Schmid G, Uberbacher R, Samaras T (2007). Radio frequency induced temperature elevations in the human head considering small anatomical structures. Radiat. Protect. Dosimetr., 124(1): 15-20.
Sliney DH, Stuck BE (1994), Microwave exposure limits for the eye: Applying infrared laser threshold data, in radiofrequency radiation standards. New York: Plenum. pp. 79-87.
Taflove A (1995). Computational Electrodynamics: The finite-difference time-domain method. Norwood, MA: Artech House.
Tinniswood AD, Furse CM, Gandhi OP (1998). Computation of SAR distributions for two anatomically based models of the human head using CAD files of commercial telephones and the parallelized FDTD code. IEEE Trans. Antennas Propagat, 46: 829-833.
Wang J, Fujiwara O (1999). FDTD computation of temperature rise in the human head for portable telephones. IEEE Trans. Microwave Theory Tech., 47:1528-1534.
Zygirdis TT, Tsiboukis TD (2008). Assessment of human head exposure to wireless communications devices: Combined electromagnetic and thermal studies for diverse frequency bands. Progress in Electromagnetics Research B., 9: 83-96.